Finite Element Arch Analysis by the Operational Method

Hiroki HAMANO* and Bennosuke TANIMOTO**
(Received October 30, 1968)

1. Introduction

Structural arches have a multitude of application in practice; hence, the analysis of arches has received the attention of a great number of investigators. The purpose of this paper is to present the operational procedure for coplanar arches by supposing that these consist of a series of small straight segments, or finite elements, each of which is governed by the ordinary longitudinal and flexural behaviors (Fig. 1). It is mentioned, therefore, that the present paper demonstrates the finite-element procedure in one dimension, and the procedure is ideally suited for such a general analysis scheme, as any arch configulation may be easily approximated as a series of simple shapes.

The loading conditions may be entirely arbitrary. Also, the curvature and the thickness of the arch may vary along its arc length.

It is well recognized that the recursive procedure in general is most efficient to digital computers, so that the present analysis requires only a little amount of labor in both programing and computer time.
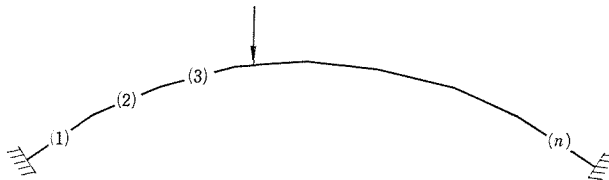

Fig. 1. Coplanar Finite Element Arch.

2. Basic Equations

The general solutions of the topological unit, namely, rectilinear beam,

---

* Senior Assistant of Civil Engineering, Faculty of Engineering, Shinshu University, Nagano, Japan.
** Professor of Civil Engineering, Faculty of Engineering, Shinshu University, Nagano, Japan.

are expressed respectively for the extensional and flexural behaviors as[1]

$$u = \lfloor\, 1 \quad \rho\,\rfloor\, \boldsymbol{M}, \tag{1}$$

and

$$w = \lfloor\, 1 \quad \rho \quad \rho^2 \quad \rho^3\,\rfloor\, \boldsymbol{N}, \tag{2}$$

in which $\rho = x/L$, $x =$ the current abscissa, $L =$ the span length, $u =$ the axial displacement, $w =$ the lateral deflection, and $\boldsymbol{M}$ and $\boldsymbol{N}$ are assemblages of integration constants. Then the behavior of the topological unit may be represented by superposition of Eqs. 1 and 2.

The complete state vector of a member is a sixth-order column matrix, consisting of the longitudinal displacement, the lateral deflection, the flexural slope, the axial force, the shearing force, and the flexural moment. Then the state vectors at any point ρ are given by the equations[2]

$$\boldsymbol{W}(\rho) = \boldsymbol{R}(\rho)\boldsymbol{X}, \tag{3}$$

and

$$\boldsymbol{W}'(\rho) = \boldsymbol{R}(\rho)[\boldsymbol{X} + \boldsymbol{K}], \tag{4}$$

in which $\boldsymbol{W}(\rho)$ and $\boldsymbol{W}'(\rho)$ hold for the normal and conjugate domains respectively. Here $\boldsymbol{R}(\rho)$ is the complete abscissa matrix of size 6-by-6, $\boldsymbol{X}$ is the sixth-order eigenmatrix which is the assemblage of integration constants, and $\boldsymbol{K}$ is the load-matrix which is compatible with any external loads.[3]

It should be noticed herein that the right sides of Eqs. 3 and 4 exhibit the complete classification of data, and then attention can be focused at attacking the eigenmatrix $\boldsymbol{X}$ only.

3. Connection Conditions and Recurrence Formula

The connection conditions are the compatibility and equiliblium at the common point of any two adjacent segments $(r - 1)$ and (r). This point is defined at point $\rho = 1$ of member $(r - 1)$ and also at point $\rho = 0$ of member (r), so that we have the following equation:

$$\boldsymbol{P}(\phi_{r-1})\boldsymbol{W}'_{r-1}(1) = \boldsymbol{P}(\phi_r)\boldsymbol{W}_r(0), \tag{5}$$

in which $\boldsymbol{P}(\phi)$ denotes the projection matrix or briefly the "projector."

Eq. 5 then will yield the desired recurrence formula, with Eqs. 3 and 4,

$$\boldsymbol{X}_r = \boldsymbol{L}_r\boldsymbol{X}_{r-1} + \boldsymbol{L}_r\boldsymbol{K}_{r-1}, \tag{6}$$

providing

$$L_r = [P(\phi_r)R_r(0)]^{-1}P(\phi_{r-1})R_{r-1}(1). \tag{7}$$

Here the L_r matrix is the shift operator or briefly the "shiftor," with which the X_{r-1} matrix can be shifted from span $(r-1)$ to the adjacent span (r). Eq. 6 is the desired recurrence formula, with which all the eigenmatrices, X_r's $(r = 2, 3, \ldots, n)$, can be expressed in terms of the first eigenmatrix, X_1. The recurrent aplication of Eq. 6 then gives

$$X_r = Q_r X_1 + \lfloor R \rfloor_{r-1}\{K\}_{r-1}, \tag{8}$$

in which

$$Q_r = L_r Q_{r-1}, \tag{9a}$$

$$\lfloor R \rfloor_{r-1} = \lfloor R_1 \quad R_2 \quad \cdots \quad R_{r-1} \rfloor_{r-1} = \lfloor L_r \lfloor R \rfloor_{r-2} \quad L_r \rfloor, \tag{9b}$$

$$\{K\}_{r-1} = \{K_1 \quad K_2 \quad \cdots \quad K_{r-1}\}. \tag{9c}$$

Note that the integrated shiftor Q_r is always a 6-by-6 square matrix, the integrated feeder $\lfloor R \rfloor_{r-1}$ is a 6-by-6$(r-1)$ rectangular matrix, and the partial assemblage of load-matrices $\{K\}_{r-1}$ is a 6$(r-1)$-by-1 column matrix.

4.   Boundary Conditions

The boundary conditions at both extreme ends of the arch are expressed by the following equations:
1.   for the left end of the arch

$$BX_1 = 0, \tag{10}$$

2.   for the right end of the arch

$$B'X_n + B'K_n = 0, \tag{11}$$

in which B and B' are the boundary matrices.

5.   Final Equation

Eq. 8 indicates that all the eigenmatrices have been expressed in terms of the single eigenmatrix X_1, so that the last step to the solution is only to determine this current eigenmatrix X_1. To do this, it will be sufficient to refer to the boundary equations, Eqs. 10 and 11.

Eq. 8 $(r = n)$ is substituted into Eq. 11, and then

$$\boldsymbol{B}'\boldsymbol{Q}_n\boldsymbol{X}_1 + \lfloor \boldsymbol{B}'\lfloor \boldsymbol{R}\rfloor_{n-1} \quad \boldsymbol{B}'\rfloor\{\boldsymbol{K}\}_n = 0. \tag{12}$$

Eqs. 10 and 12 are put into one equtaion, from which $\boldsymbol{X}_1$ can be found to be

$$\boldsymbol{X}_1 = -\begin{bmatrix} \boldsymbol{B} \\ \boldsymbol{B}'\boldsymbol{Q}_n \end{bmatrix}^{-1}\begin{bmatrix} \boldsymbol{O} \\ \boldsymbol{B}'\lfloor \boldsymbol{R}\rfloor_{n-1} \quad \boldsymbol{B}' \end{bmatrix}\{\boldsymbol{K}\}_n, \tag{13}$$

which is the desired final equation. Eq. 13 takes the form

$$\boldsymbol{X}_1 = \lfloor \boldsymbol{G}\rfloor\{\boldsymbol{K}\}_n, \tag{14}$$

of which the $\lfloor \boldsymbol{G}\rfloor$ matrix is of the size 6-by-$6n$ and the $\{\boldsymbol{K}\}_n$ matrix is of the size $6n$-by-1. The former, $\lfloor \boldsymbol{G}\rfloor$, depends on only the geometry and material properties of the arch, and hence it is called the "geometry matrix." The latter, $\{\boldsymbol{K}\}_n$, is the assemblage of all the load-matrices.

6. Numerical Examples

Some numerical examples of the preceding arch analysis will be given. Here the geometry and material properties of the arch are taken to be as follows:

Table 1.

E (t/m^2)	I (m^4)	A (m^2)	L (m)	h (m)
21 000 000.0	0.005	0.04	36.0	3.0

in which E = Young's modulus, I = the moment of inertia of the cross section, A = the cross-sectional area, L = the span length of the arch, and h = the rise of the arch; all the constants being measured with the ton-meter unit. In the following examples, each result gives the complete state vector for the axial and lateral behaviors of the arch. The values of the state vector components are for convenience taken to be the mean values of the end values of two adjacent rectilinear finite elements.

(a) Example 1.—Fig. 2

As the arch is divided into finer elements, the results obtained will tend to the rigorous solution. Table 2 shows the numerical results of the flexural deflection and the moment, w and M, at the loaded point (2) for the 4, 8, 16, 32, and 64 divided finite element arch, which shows a rapid convergence to the rigorous solution. It will be seen that the 16 or 32 finite element arch will

suffice the practical purpose. The values corresponding to the infinitely great number finite element arch are due to the rigorous solution computed by the known theory (cf. Additional Note).

Table 2.

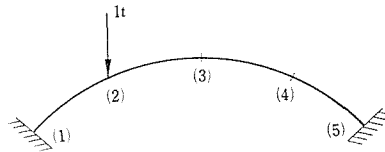|	$w \times 10^4$(m)	M (t$-$m)
4	3.928	2.001
8	3.967	2.137
16	3.975	2.171
32	3.976	2.179
64	3.977	2.182
∞	3.977	2.182

Fig. 2. Circular Arch with Both Ends Clamped.

Table 2 shows the state vector for each point (Fig. 2) at the 64 divided finite element arch.

Table 3. State Vector for Each Point (Fig. 2).

	$u \times 10^4$ (m)	$w \times 10^4$ (m)	$\theta \times 10^4$	F (t)	S (t)	M (t)
(1)	0.0	0.0	0.0	-1.552	0.370	-2.295
(2)	0.132	3.977	0.216	-1.393	0.605 -0.367	2.182
(3)	0.488	1.072	-0.485	-1.352	-0.154	-0.241
(4)	0.252	-1.284	0.040	-1.359	0.071	-0.621
(5)	0.0	0.0	0.0	-1.331	0.286	1.052

(b) Example 2. —Table 4

As the second example, four types of arches are evaluated, and the numerical results are given in table 4. Each of the state vector components has two numerical values; the upper case referring to the 32 finite element arch, while the lower one to the 64 finite element arch. It is seen that these two values closely approximate each other, and hence they are practically accurate.

Table 4. Four Types of Arches.

No.	Types		$u \times 10^4$ (m)	$w \times 10^4$ (m)	$\theta \times 10^4$	F (t)	S (t)	M (t—m)
1	Circular arch with both ends clamped	(1)	0.0	0.0	0.0	−2.466	−0.290	0.392
			0.0	0.0	0.0	−2.465	−0.303	0.396
		(2)	−0.238	1.047	0.373	−2.481	0.093	−0.630
			−0.238	1.047	0.373	−2.481	0.093	−0.626
		(3)	0.0	4.601	0.0	−2.432	0.500 −0.500	2.095
			0.0	4.600	0.0	−2.432	0.500 −0.500	2.099
2	Circular arch with both ends hinged	(1)	0.0	0.0	−0.129	−2.315	−0.240	0.0
			0.0	0.0	−0.130	−2.312	−0.252	0.0
		(2)	−0.255	0.881	0.413	−2.324	0.120	−0.664
			−0.256	0.880	0.413	−2.323	0.120	−0.661
		(3)	0.0	4.702	0.0	−2.273	0.500 −0.500	2.182
			0.0	4.704	0.0	−2.271	0.500 −0.500	2.186
3	Parabolic arch with both ends clamped	(1)	0.0	0.0	0.0	−2.465	−0.271	0.359
			0.0	0.0	0.0	−2.464	−0.282	0.363
		(2)	−0.239	1.078	0.371	−2.478	0.094	−0.606
			−0.240	1.078	0.371	−2.478	0.094	−0.603
		(3)	0.0	4.520	0.0	−2.429	0.500 −0.500	2.072
			0.0	4.520	0.0	−2.429	0.500 −0.500	2.075
4	Parabolic arch with both ends hinged	(1)	0.0	0.0	−0.120	−2.326	−0.226	0.0
			0.0	0.0	−0.121	−2.323	−0.236	0.0
		(2)	−0.254	0.922	0.408	−2.334	0.118	−0.636
			−0.255	0.921	0.409	−2.332	0.118	−0.633
		(3)	0.0	4.606	0.0	−2.283	0.500 −0.500	2.152
			0.0	4.607	0.0	−2.281	0.500 −0.500	2.156

(c) **Example 3.—Table 5**

When the span length of the arch is 36 meters and the arch rise is 3, 6, and 9 meters respectively, the horizontal reaction, H, at the left bounding end results in the values given in Table 5.

Table 5. Horizontal Reaction (32 Finite Element Arch, Fig. 3).

Applied point	Horizontal reaction H (t)		
of load $P = 1$(t)	$h = 3^{m}$ $h/L = \dfrac{1}{12}$	$h = 6^{m}$ $h/L = \dfrac{1}{6}$	$h = 9^{m}$ $h/L = \dfrac{1}{4}$
(1)	0.867	0.411	0.242
(2)	1.606	0.785	0.489
(3)	2.100	1.045	0.673
(4)	2.273	1.138	0.740
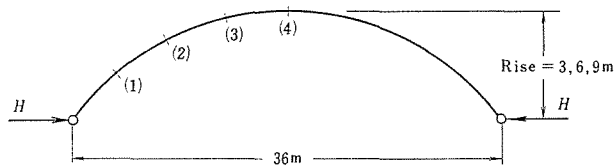
Fig. 3. Circular Arch with Both Ends Clamped.

(d) **Example 4. —Table 6**

Table 6 shows the generalized force of the arch at three points indicated in the figures in the table, the left being the uniform cross-sectional parabolic arch with 0.9 meter constant depth, while the right the variable cross-sectional parabolic arch with 1.2 meters depth at both extreme ends and 0.6 meter depth at the crown with linear change of depth. The values of the stresses (f, τ, σ) are computed by the formula

$$f = \frac{F}{A}, \qquad \tau = \frac{S}{A}, \qquad \sigma = \frac{M\,a}{I\,2}, \tag{15}$$

in which $f = $ the normal stress due to the resultant axial force, $\tau = $ the average shearing stress, $\sigma = $ the extreme fiber stress due to flexure, and $a = $ the depth of the cross section. The width of both arches is 0.6 meter, the span length is 36 meters, the rise is 4.5 meters, and Young's modulus is 2 100 000 ton per sq meter.

Table 6. Parabolic Arches.

	Uniformly cross-sectional parabolic arch with both ends clamped			Variable cross-sectional parabolic arch with both ends clamped		
	Generalized force					
	F (t)	S (t)	M (t−m)	F (t)	S (t)	M (t−m)
(1)	−1.836	−0.334	0.892	−1.877	−0.353	1.026
(2)	−1.865	0.049	−0.676	−1.909	0.038	−0.695
(3)	−1.798	0.500 −0.500	1.802	−1.843	0.500 −0.500	1.732
	Stresses					
	f (t/m²)	τ (t/m²)	σ (t/m²)	f (t/m²)	τ (t/m²)	σ (t/m²)
(1)	−3.400	−0.619	11.012	−2.607	−0.490	7.125
(2)	−3.454	0.091	−8.346	−3.535	0.070	−8.580
(3)	−3.330	0.926 −0.926	22.247	−5.119	1.389 −1.389	48.111

7. Further Developments

The present investigation can be extended to any structural systems involving arch members. The arch box frame resting on an elastic foundation (Fig. 4) and the continuous arch portal frame (Fig. 5) have been analyzed.
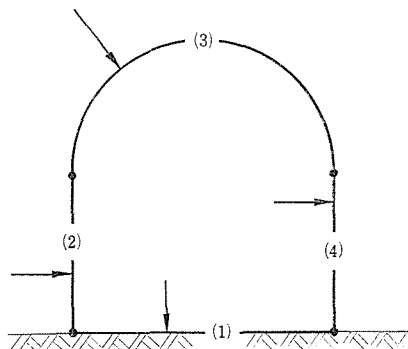

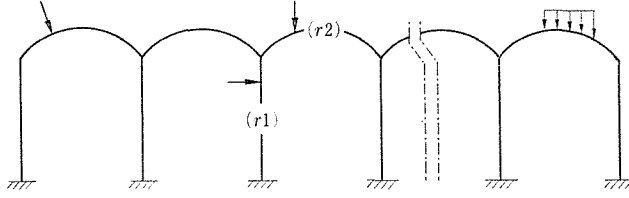**Fig. 4. Arch Box Frame on Elastic Foundation.**

Fig. 5.   Continuous Arch Portal Frame.

8.   Additional Note

The circular arch is governed by the equations[4]

$$F = \frac{EA}{R}\left(\frac{du}{d\phi} - w\right), \tag{16}$$

$$M = -\frac{EI}{R^2}\left(\frac{d^2w}{d\phi^2} + \frac{du}{d\phi}\right), \tag{17}$$

in which R = the radius of the arch, and ϕ = the angular parameter of the arch. These two equations give the general solution

$$\begin{bmatrix} u \\ w \end{bmatrix} = \begin{bmatrix} 1 & \phi & \cos\phi & \sin\phi & \phi\cos\phi & \phi\sin\phi \\ 0 & 1 & -\sin\phi & \cos\phi & \beta\cos\phi - \phi\sin\phi & \beta\sin\phi + \phi\cos\phi \end{bmatrix} \boldsymbol{X}, \tag{18}$$

in which

$$\beta = \frac{AR^2 - I}{AR^2 + I}. \tag{19}$$

Hence, the complete state vector becomes

$$\boldsymbol{W}(\psi) = \boldsymbol{R}(\psi)\boldsymbol{X}. \tag{20}$$

The eigenmatrix $\boldsymbol{X}$ is then found by the equation[5]

$$\boldsymbol{X} = -\begin{bmatrix} \boldsymbol{B} \\ \boldsymbol{B'} \end{bmatrix}^{-1} \begin{bmatrix} 0 \\ \boldsymbol{B'} \end{bmatrix} \boldsymbol{K}, \tag{21}$$

in which, as before, $\boldsymbol{B}$ and $\boldsymbol{B'}$ denote boundary matrices at both ends of the arch, and $\boldsymbol{K}$ represents the load-matrix.

9. Conclusions

This paper presents the operational finite element method, which is applicable to the analysis of structural arches. It permits recurrence avoiding large-size simultaneous equations. Effects of temperature changes, movements of supports, and any distributions of applied loads can be treated by the method presented.

Acknowledgements

References

1) N. YOSHIZAWA and B. TANIMOTO, "Operational Method for Structural Networks, First Report, Plane Systems with Rigid Connection," Journal of the Faculty of Engineering, Shinshu University, Nagano, Japan, Vol. 21, June, 1966, p. 23.

2) S. NATSUME, N. YOSHEIZAWA, H. HAMANO, and B. TANIMOTO, "Direct Analysis of Continuous Beam-Columns," Journal of the Faculty of Engineering, Shinshu University, Nagano, Japan, Vol. 23, Feb., 1967, pp. 2–3.

3) N. YOSHEZAWA and B. TANIMOTO, "Operational Method for Continuous Beams, Second Report, Generalized Continuous Beams," Journal of the Faculty of Engineering, Shinshu University, Nagano, Japan, Vol. 20, June, 1966, p. 33.

4) S. TIMOSHENKO, "Strength of Materials," Part I, Third Edition, D. Van Nostrand Co., Inc., 1955, pp. 401–405.

5) B. TANIMOTO, "Some Improvements on Proposed Eigen-Matrix Method," Proceeding of the ASCE, Structural Division, Feb., 1966, p. 103.

Appendix. —Notation

The following symbols are used in this paper:

A	= cross-sectional area;
a	= depth of the cross section; Eq. 15;
B, **B'**	= boundary conditions at extreme left and right ends respectively; Eqs. 10 and 11;
EI	= flexural rigidity;
F	= axial force;
f	= normal stress due to the resultant axial force; Eq. 15;
$\lfloor G \rfloor$	= geometry matrix; Eq. 14;
H	= horizontal reaction; Ex. 3;

h	= rise of the arch;
$\boldsymbol{K}$	= load-matrix; Eq. 4;
$\{\boldsymbol{K}\}$	= load-matrix assemblage; Eq. 12;
L	= span length of the arch;
$\boldsymbol{L}$	= shiftor; Eq. 7;
M	= bending moment;
$\boldsymbol{M}$	= 2-by-1 eigenmatrix; Eq. 1;
$\boldsymbol{N}$	= 4-by-1 eigenmatrix; Eq. 2;
P	= lateral concentrated load;
$\boldsymbol{P}(\phi)$	= projector; Eq. 5;
$\boldsymbol{Q}$	= integrated shiftor; Eq. 9a;
R	= radius of the circular arch; Eq. 16;
$\boldsymbol{R}(\rho)$	= abscissa matrix; Eq. 3;
$\lfloor \boldsymbol{R} \rfloor$	= integrated feeder; Eq. 9b;
S	= shearing force;
u	= axial displacement; Eq. 1;
$\boldsymbol{W}(\rho)$, $\boldsymbol{W}'(\rho)$	= state vector for normal and conjugate domain respectively; Eqs. 3 and 4;
w	= lateral deflection; Eq. 2;
$\boldsymbol{X}$	= 6-by-1 eigenmatrix; Eq. 3;
x	= current abscissa;
β	$= (AR^2 - I)/(AR^2 + I)$;
θ	= flexural slope;
ρ	$= x/L$, dimensionless current abscissa; Eqs. 1 and 2;
σ	= extreme fiber stress due to flexure; Eq. 15;
τ	= average shearing stress; Eq. 15;
ϕ	= local intersection angle between two consecutive straight finite elements; Eq. 5;
ψ	= angular parameter of the circular arch; Eqs. 16 and 17;
$\lfloor \ \ \rfloor$	= row vector; and
$\{ \ \ \}$	= column vector.